

## Bis-[(5-amino-1*H*-1,2,4-triazol-3-yl)mercapto]alkanes – novel twin compounds as copper corrosion inhibitors in high chloride containing media

A.A. Kruzhilin,<sup>1</sup> D.S. Shevtsov,<sup>1</sup> D.V. Lyapun,<sup>1</sup> A.Yu. Potapov,<sup>1</sup>  
O.A. Kozaderov,<sup>1</sup> E.V. Nikitina<sup>2</sup> and Kh.S. Shikhaliev<sup>1</sup>\*

<sup>1</sup>Voronezh State University, 1 Universitetskaya pl., 394018 Voronezh, Russian Federation

<sup>2</sup>Peoples' Friendship University of Russia (RUDN University), 6 Miklukho-Maklaya St.,  
117198 Moscow, Russian Federation

\*E-mail: [shikh1961@yandex.ru](mailto:shikh1961@yandex.ru)

### Abstract

The article describes an example of application of the twin molecule concept in the molecular design of new organic corrosion inhibitors. We have developed a synthesis method and proved the structure of new bis-[(5-amino-1*H*-1,2,4-triazol-3-yl)mercapto]alkanes as a result of the condensation of 3-mercapto-5-amino-1,2,4-triazole with dihaloalkanes. The inhibitory effect of the synthesized substances on copper corrosion in neutral and acidic chloride-containing media was evaluated using direct tests in a salt-spray chamber and weight loss measurements as well as potentiodynamic polarization measurements. It has been established that bis-[(5-amino-1*H*-1,2,4-triazol-3-yl)mercapto]alkanes **A–C** at a concentration of at least 0.10 mmol · dm<sup>-3</sup> show high protective characteristics both in direct tests (from 64 to 192 h in salt spray and from 92 to 99% in 1 wt.% HCl solutions) and in electrochemical tests (from ~30 to ~85% in 10 mM NaCl solutions). Moreover, the degree of protection increases smoothly with an increase in the concentration of the inhibitor, as well as with an increase in the length of the linker hydrocarbon fragment. These developed compounds can be used to protect various heat exchange equipment made of copper or its alloys. They are promising for use in water circulation systems to prevent corrosion and scale formation, as well as to protect copper in the production of conductor materials, to prevent or slow down atmospheric corrosion of structural materials based on copper and its alloys. The developed compounds can be used to protect various heat exchange equipment made of copper or its alloys, are promising for use in water circulation systems to prevent corrosion and scale formation, in the protection of copper in the production of conductor materials, to prevent or slow down atmospheric corrosion of construction materials based on copper and its alloys.

Received: February 28, 2023. Published March 10, 2023

doi: [10.17675/2305-6894-2023-12-1-14](https://doi.org/10.17675/2305-6894-2023-12-1-14)

**Keywords:** copper, corrosion inhibitors, chlorides, triazole derivatives, bis-triazolyl-mercapto-alkanes.

## 1. Introduction

Copper and its alloys are widely used as a material for heat exchange equipment, as constructional, roofing, plumbing materials, as well as conductors and various components of electrical equipment in the fields of construction, transport, energy, microelectronics, light and heavy industry, *etc.* One of the common approaches to reducing corrosion damage is the use of corrosion inhibitors. Corrosion inhibitors provide corrosion resistance to copper and its alloys in these industries against factors such as weather conditions, humidity, increased chloride content, petroleum products, high temperatures, aggressive gases, aggressive chemicals, and aggressive liquids. Azoles and their derivatives have found the widest application in protecting copper and its alloys from corrosion [1–4].

Recently, more attention has been paid to them, as successful selection of substituents can expand or, conversely, specify the application range of the obtained inhibitor [5–7].

In addition, it is well known that the presence of lyophilic and hydrophobic groups in the inhibitor structure promotes the process of its adsorption on the electrode surface [8–10]. Thus, a number of publications have been devoted to the study of the inhibiting activity in an acidic environment of some traditional surfactants consisting of a single head group and a single hydrophobic group [11–15]. In recent decades, new classes of surfactant molecules have become widespread in industrial and research areas. One of such classes is gemini surfactants, which have two hydrophilic head groups and two hydrophobic groups per molecule separated by a spacer [16–18]. It is known that such surfactants have some important properties (such as very low critical micelle concentration, high solubilizing capacity, increased stability to destruction, *etc.*) compared to corresponding conventional surfactants [19].

In light of these considerations, this study demonstrates the possibility of obtaining and investigating the anticorrosive properties of new cross-linked molecules of azole class corrosion inhibitors similar to gemini surfactants. This concept is not new, and there are studies in this direction; however, such studies are usually limited to investigating existing gemini surfactants as corrosion inhibitors [20, 21], while studies of heterocyclic inhibitors with similar twin structures are few in number.

In early studies, we synthesized and studied a series of various derivatives of 5-amino-1,2,4-triazole containing various aliphatic, alicyclic, aromatic, and heterocyclic substituents in their structure. The matrix of 5-amino-1,2,4-triazole provides effective adsorption of the inhibitor molecule on the metal surface. The mechanism and nature of the formation of such adsorbed inhibitor layers remain not fully understood. However, the results of numerous tests of derivatives of this class, including those described in our earlier studies [22, 23], confirm their high efficiency in inhibiting corrosion of non-ferrous and ferrous metals under conditions of chloride corrosion in neutral or acidic environments. The use of the twin-molecule concept in the molecular design of new triazole derivatives appears to us as a promising but understudied direction, both in terms of synthesis and in the investigation of their anticorrosive activity. Considering the previously identified high anticorrosive activity

of 3-alkylmercapto-5-amino-1*H*-1,2,4-triazoles, we set out to study the targeted synthesis of bis-[(5-amino-1*H*-1,2,4-triazol-3-yl)mercapto]alkanes by condensing 3-mercapto-5-amino-1,2,4-triazole with dihaloalkanes and to investigate their inhibitory effect on copper in high chloride containing media.

## 2. Experimental

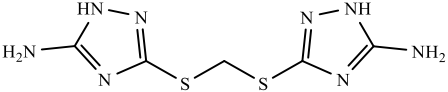
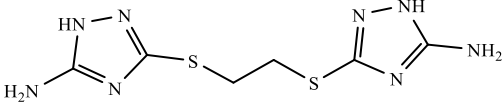
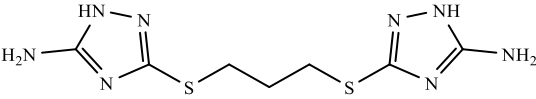
### 2.1. Methods for analyzing the chemical structure of inhibitors

Aminotriazoles were analyzed by high performance liquid chromatography with high resolution mass spectrometric detection using electrospray ionization (HPLC-HRMS-ESI) combined with UV detection. The device consisted of an Agilent 1269 Infinity liquid chromatograph and an Agilent 6230 TOF LC/MS high-resolution time-of-flight mass detector. Quantitative determination was performed by the internal standard method. <sup>1</sup>H NMR spectra were recorded on a Bruker AV600 spectrometer (600.13 MHz) in DMSO-d<sub>6</sub>, TMS was the internal standard. The IR spectrum was recorded on a Vertex 70 IR-Fourier spectrometer using a Platinum ATR (Bruker) ATR attachment equipped with a diamond prism in the frequency range from 4000 to 400 cm<sup>-1</sup> with a resolution of 2 cm<sup>-1</sup>. The result is obtained by averaging 16 scans.

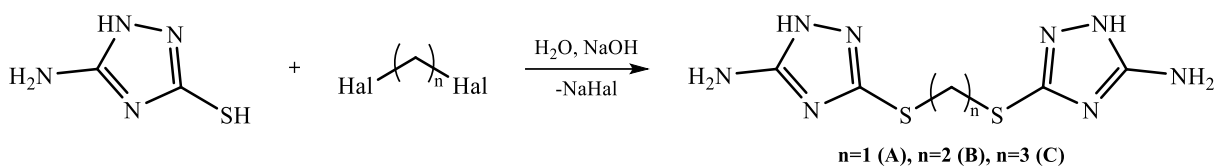
### 2.2. Synthesis and analysis of inhibitors

As inhibitors of copper chloride corrosion, a series of new previously unstudied bis-[(5-amino-1*H*-1,2,4-triazol-3-yl)mercapto]alkanes was obtained (Table 1).

**Table 1.** List of studied inhibitors.

Symbol	Name	Formula
A	1,1-(bis-[(5-amino-1 <i>H</i> -1,2,4-triazol-3-yl)mercapto])methane	
B	1,2-(bis-[(5-amino-1 <i>H</i> -1,2,4-triazol-3-yl)mercapto])ethane	
C	1,3-(bis-[(5-amino-1 <i>H</i> -1,2,4-triazol-3-yl)mercapto])propane	

It has been established that the interaction of such dihaloalkanes as methylene iodide, 1,2-dibromobutane, and 1,3-dibromopropane with the sodium salt of 3-mercapto-5-amino-1,2,4-triazole in a molar ratio of 2:1 exclusively yields the twin 1,1-(bis[(5-amino-1*H*-1,2,4-triazol-3-yl)mercapto])methane **A**, 1,2-(bis[(5-amino-1*H*-1,2,4-triazol-3-yl)mercapto])ethane **B**, and 1,3-(bis[(5-amino-1*H*-1,2,4-triazol-3-yl)mercapto])propane **C**.



*General procedure for the synthesis of 1,3-bis-[(5-amino-1H-1,2,4-triazol-3-yl)mercapto]alkanes A–C.*

In a conical flask, 0.13 moles of 3-mercapto-5-amino-1H-1,2,4-triazole were dissolved in a solution containing 5.3 g of sodium hydroxide in 40 ml of water. Then, while stirring the resulting mass intensively at no less than 500 rpm, 0.065 moles of the corresponding dihaloalkane-methylene iodide, 1,2-dibromoethane or 1,3-dibromopropane, were added dropwise over 3 hours at a rate of ~5 drops per minute. The mixture was stirred for 5–10 hours depending on the activity of the alkylating agent. The precipitate formed was filtered off, washed with water, and recrystallized from water.

*1,1-bis-[(5-amino-1H-1,2,4-triazol-3-yl)mercapto]methane A.* Yield 75%, white solid, m.p. 191–193°C. <sup>1</sup>H NMR spectrum 4.60 (s, 2H, CH<sub>2</sub>), 6.12 (s, 2H, NH<sub>2</sub>), 12.02 (s, H, NH). IR spectrum: 3276, 3305, 3346 (NH<sub>2</sub>, NH). Found, *m/z*: 245.0389 [M+H]<sup>+</sup>. C<sub>5</sub>H<sub>8</sub>N<sub>8</sub>S<sub>2</sub>. Calculated, *m/z* 245.0386.

*1,2-bis-[(5-amino-1H-1,2,4-triazol-3-yl)mercapto]ethane B.* Yield 80%, white solid, m.p. 213–215°C. <sup>1</sup>H NMR spectrum: 3.68 (s, 4H, 2CH<sub>2</sub>), 6.20 (s, 4H, NH<sub>2</sub>), 12.02 (s, 2H, NH). IR spectrum: 3275, 3300, 3351 (NH<sub>2</sub>, NH). Found, *m/z*: 259.0537 [M+H]<sup>+</sup>. C<sub>6</sub>H<sub>10</sub>N<sub>8</sub>S<sub>2</sub>. Calculated, *m/z* 259.0543.

*1,3-bis-[(5-amino-1H-1,2,4-triazol-3-yl)mercapto]propane C.* Yield 79%, white solid, m.p. 202–204°C. <sup>1</sup>H NMR spectrum: 1.94–1.98 (m, 2H, CH<sub>2</sub>), 3.01 (t, 4H, 2SCH<sub>2</sub>), 6.03 (s, 4H, 2NH<sub>2</sub>), 11.91 (s, 2H, 2NH). IR spectrum: 3277, 3306, 3347 (NH<sub>2</sub>, NH). Found, *m/z*: 273.0694 [M+H]<sup>+</sup>. C<sub>7</sub>H<sub>12</sub>N<sub>8</sub>S<sub>2</sub>. Calculated, *m/z* 273.0699.

To evaluate the protective effect of the synthesized compounds (A–C), a complex of electrochemical and direct corrosion tests was used.

### 2.3. Potentiodynamic polarization measurements

Electrochemical measurements were performed at room temperature (~25°C) on copper (M1) electrodes in an unstirred borate buffer aqueous solution (pH 7.4) with natural aeration, in the presence of the inhibitor and 10 mM NaCl. A classical electrolytic three-electrode cell without separation of anode and cathode compartments was used in order to accelerate transient measurements.

A saturated silver chloride reference electrode was placed in a separate container linked to the electrolytic cell by an agar-agar-based salt bridge filled with a potassium nitrate saturated solution. The auxiliary electrode was a platinum gauze. The working copper electrode was polished by K3000 sandpaper, degreased in 96% ethanol, and washed with

distilled water. The potentials of the working electrode ( $E$ ) are given according to the standard hydrogen electrode (SHE) scale. The current density  $i$  was calculated by dividing the actual current  $I$  by the geometric area of the working electrode ( $0.75 \text{ cm}^2$ ).

Electrochemical measurements were performed using an IPC-PRO potentiostat. In order to remove an oxide film, the working Cu-electrode was cathodically pre-polarized at  $E = -0.60 \text{ V}$  for 15 minutes prior to the experiment. The electrode was then held in the solution for about 3 to 5 minutes until the corrosion potential ( $E_{\text{cor}}$ ) stabilized. A NaCl solution was then added to the working solution while stirring, so that the concentration of chloride ions would be  $C_{\text{Cl}^-} = 10 \text{ mM}$ . The studied inhibitors were also added to the solution in the concentration of  $C_{\text{inh}} = 0.01, 0.10$  and  $1.00 \text{ mM}$ . After the new  $E_{\text{cor}}$  value was established, the polarization curve was registered by scanning the potential towards either the anode or the cathode at  $0.2 \text{ mV/sec}$ . The activation potential ( $E_{\text{act}}$ ) was identified by a rapid increase in the current on the anode polarization curve. Pits were then visually identified on the surface of the electrode. The measurement error for  $E_{\text{act}}$  was below  $0.03 \text{ V}$ .

The rate of corrosion in current units ( $i_{\text{cor}}$ ) was determined by the polarization resistance technique as summarized by Mansfeld [24].

The effectiveness of the inhibition activity of the bis-[(5-amino-1H-1,2,4-triazol-3-yl)mercapto]alkanes was evaluated by the degree of protection

$$Z_i = \frac{i_{\text{cor},0} - i_{\text{cor,inh}}}{i_{\text{cor},0}} \times 100\% ,$$

where  $i_{\text{cor},0}$  and  $i_{\text{cor,inh}}$  are the corrosion current densities with and without an inhibitor respectively.

#### 2.4. Direct corrosion tests

Direct corrosion tests were carried out on copper plates  $20 \times 50 \times 0.10 \text{ mm}$  in size, which were pre-polished with K3000 sandpaper and degreased with acetone.

The experiments, which lasted  $t = 7$  days, were carried out on three samples in an unstirred naturally aerated 1% HCl solution. The plates were then washed with distilled water and treated according to GOST 9.907-83 “Methods for the removal of corrosion products after corrosion tests”. The corrosion rate was determined according to the weight loss of the samples and calculated using the equation:

$$k_{\text{inh}} = \frac{m_0 - m}{S \times t} ,$$

where  $m_0$  and  $m$  is the weight of the sample before and after the corrosion tests respectively,  $S$  – summarized area of the plate,  $\text{m}^2$ ,  $t$  – experiment time, days.

The inhibition efficiency was evaluated by the value of the degree of protection:

$$Z_k = \frac{k_0 - k_{\text{inh}}}{k_0} \times 100\% ,$$

where  $k_0$  and  $k_{\text{inh}}$  are the rates of corrosion in the HCl solution with and without the inhibitor respectively. The parameter  $k_0$  was  $\sim 19.2 \text{ g}\cdot\text{m}^{-2}\cdot\text{day}^{-1}$ .

Atmospheric corrosion of copper was accelerated by a salt spray test to determine the effectiveness of inhibition of bis-[(5-amino-1*H*-1,2,4-triazol-3-yl)mercapto]alkanes in the inter-operation protection of copper products. Protective inhibitor films were obtained by keeping copper plates in an aqueous solution with an inhibitor for 60 minutes at 60°C. The samples were wiped with filter paper and air-dried at room temperature for 2 hours. Then, they were placed into a sealed chamber with a volume of 14000 cm<sup>3</sup> and 95–100% humidity. A 5% solution of NaCl was sprayed into the chamber using a pump with 6 hydraulic nozzles, which were automatically turned on for 1 second every hour (the solution flow rate per nozzle was approximately 7 ml). The samples were examined 3 times every 24 hours in order to establish the time of appearance of the first signs of corrosion ( $\tau_{\text{cor}}$ ).

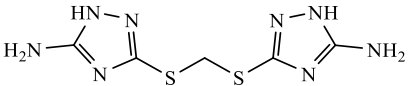
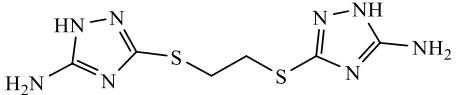
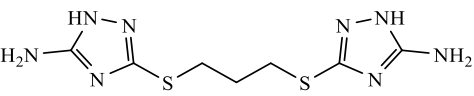
### 3. Results and Discussion

#### 3.1. Direct corrosion tests

The results of direct tests are the closest approximation to the real corrosion conditions and best reflect the effectiveness of the studied inhibitors in their actual use. It was found that the average protection degree of all tested substances was >90%. The minimum value was 75% for inhibitor **A** at a concentration of 0.01 mmol·dm<sup>-3</sup> in the test solution. It should be noted that all investigated inhibitors are limited soluble in aqueous chloride-containing solutions, but their maximum efficiency is observed at  $C_{\text{inh}}=0.10 \text{ mmol}\cdot\text{dm}^{-3}$ . Such inhibitor concentration is achievable for all investigated compounds, and therefore the solubility issue does not affect the effectiveness of the developed bis-triazolyl-mercaptoalkanes.

Salt spray test results were generally consistent with weight loss measurements. At the same time, the time of appearance of the first signs of corrosion on copper plates treated with 1,3-bis[(5-amino-1*H*-1,2,4-triazol-3-yl)mercapto]propane **C** solution was 2–3 times longer than for methane and ethane derivatives. This is probably due, on the one hand, to the increase in the length of the aliphatic chain that crosslinks the mercaptotriazole cycles and, on the other hand, to the lower solubility of derivative **C**, which makes its desorption from the metal surface more difficult and, consequently, provides longer protection of the latter.

**Table 2.** Results of anticorrosion tests of bis-[(5-amino-1*H*-1,2,4-triazol-3-yl)mercapto]alkanes by gravimetric and salt spray test methods.

Inhibitor	$C_{inh}$ , $\text{mmol} \cdot \text{dm}^{-3}$	$k_{inh}$	$Z_k$ , %	$\tau_{cor}$ , h
<b>None</b>	–	19.2	–	2
 <b>A</b>	0.01	4.8	75.0	48
	0.10	0.9	95.3	64
	1.00	0.2	99.0	66
 <b>B</b>	0.01	3.6	81.3	48
	0.10	1.4	92.7	54
	1.00	1.2	93.8	70
 <b>C</b>	0.01	1.2	93.8	169
	0.10	0.5	97.4	192

### 3.2. Potentiodynamic polarization measurements

In continuation of the study, potentiodynamic measurements were carried out to record the full anodic and cathodic polarization curves and evaluate the corrosion current density ( $i_{cor}$ ) in a borate buffer with NaCl addition in the presence of studied inhibitors.

It has been found that the addition of the studied concentrations of 1,1-bis[(5-amino-1*H*-1,2,4-triazol-3-yl)mercapto]methane **A** results in a shift of the corrosion potential,  $E_{corr}$ , towards the cathodic region by 30–60 mV relative to the control experiment. At the initial stages of the anodic polarization curves, a decrease in the current density relative to the control experiment was observed up to the potential region of  $\sim +200$ – $220$  mV for all studied concentrations. At concentrations of  $0.01$ – $0.10$   $\text{mmol} \cdot \text{dm}^{-3}$ , an increase in the anodic current density was observed upon further polarization beyond 200 mV, which exceeded the control value by  $\sim 1.5$ – $2$  times at the maximum point. The position of the maximum of anodic current density on the potential axis is  $\sim +300$ – $320$  mV. After reaching the maximum, the current decreased to  $5.3$   $\mu\text{A}$  and then sharply increased. The pitting potential, at which the anodic current sharply increased, was shifted towards the cathodic region by  $\sim +120$ – $130$  mV relative to the control experiment. At an additive concentration of  $1.00$   $\text{mmol} \cdot \text{dm}^{-3}$ , no current maximum was formed. The pitting potential was shifted by  $+30$  mV relative to the control. Therefore, a significant influence on the anodic half-reaction was observed at a concentration of at least  $1$   $\text{mmol} \cdot \text{dm}^{-3}$ . At inhibitor concentrations of  $0.10$  and  $1.00$   $\text{mmol} \cdot \text{dm}^{-3}$ , the corrosion current density value near the free corrosion potential was reduced relative to the control. The degree of protection according to the polarization resistance method was approximately 30% and 84%, respectively.

On the cathodic polarization curves, at inhibitor concentrations of at least  $0.10$   $\text{mmol} \cdot \text{dm}^{-3}$ , an expansion of the region of small cathodic currents (the polarization

curve was close to the zero axis of currents) was observed. The position of the region of increasing cathodic current density was found to be shifted towards the cathodic region by  $-50$  mV and  $-150$  mV, respectively, relative to the control experiment. Therefore, at a concentration of  $0.10 \text{ mmol} \cdot \text{dm}^{-3}$ , 1,1-bis[(5-amino-1*H*-1,2,4-triazol-3-yl)mercapto]methane can act as a cathodic inhibitor, and at a concentration of at least  $1 \text{ mmol} \cdot \text{dm}^{-3}$ , as a mixed inhibitor.

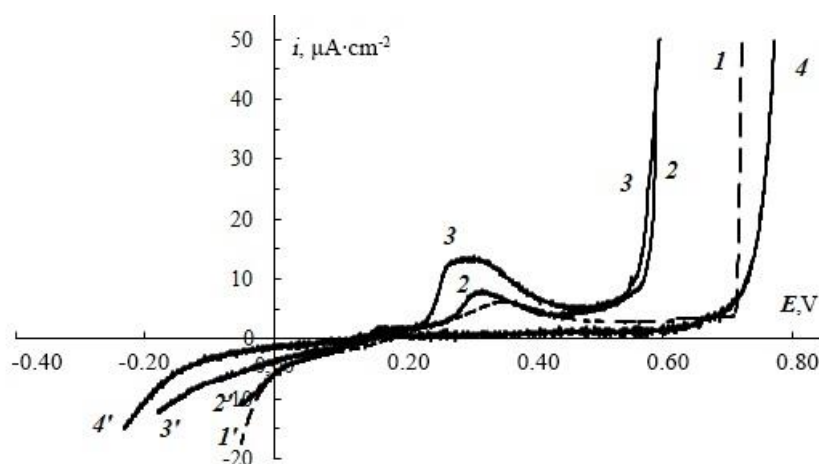
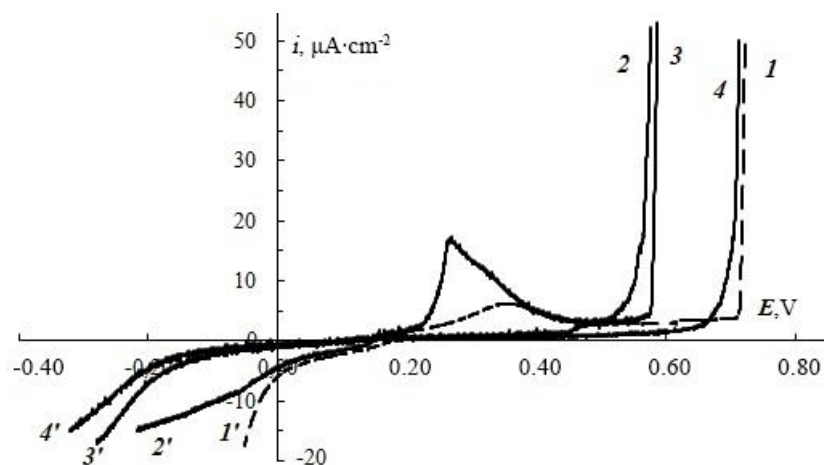


**Figure 1.** Anodic ( $I-4$ ) and cathodic ( $I'-4'$ ) polarization curves of copper in borate buffer ( $\text{pH}=7.40$ ) with  $10 \text{ mM NaCl}$  and 1,1-bis-[(5-amino-1*H*-1,2,4-triazol-3-yl)mercapto]methane (**A**) at concentrations  $C_{\text{inh}}$  ( $\text{mmol} \cdot \text{dm}^{-3}$ ): 1,  $I'$  – without an inhibitor; 2,  $2'$  –  $0.01$ ; 3,  $3'$  –  $0.10$ ; 4,  $4'$  –  $1.00$ .

In the presence of  $0.01 \text{ mmol} \cdot \text{dm}^{-3}$  of 1,2-bis[(5-amino-1*H*-1,2,4-triazol-3-yl)mercapto]ethane **B**, the free corrosion potential,  $E_{\text{corr}}$ , shifts by  $20$  mV towards the cathodic region relative to the control experiment. At additive concentrations of  $0.10 \text{ mmol} \cdot \text{dm}^{-3}$  and  $1.00 \text{ mmol} \cdot \text{dm}^{-3}$ ,  $E_{\text{corr}}$  was shifted towards the anodic region by  $55$  mV relative to the control experiment. At an inhibitor concentration of  $0.01 \text{ mmol} \cdot \text{dm}^{-3}$ , the potential shift of  $50$  mV relative to  $E_{\text{corr}}$  was accompanied by a sharp increase in the anodic current density, which at the maximum point ( $i=16 \text{ } \mu\text{A} \cdot \text{cm}^{-2}$  at  $E \sim +270$  mV) was three times higher than the control value. The maximum was found to be shifted by  $-50$  mV relative to the control experiment. After the maximum, the current decreases and remains constant up to the activation potential of  $\sim +550$  mV (approximately  $180$  mV more positive than the control experiment). At inhibitor concentrations of  $0.10 \text{ mmol} \cdot \text{dm}^{-3}$  and above, no maximum anodic current was formed. The current density remains constant up to activation potentials of  $\sim +580$  mV and  $\sim +700$  mV for concentrations of  $0.10 \text{ mmol} \cdot \text{dm}^{-3}$  and  $1.00 \text{ mmol} \cdot \text{dm}^{-3}$ , respectively. The passivation current density is three times lower than that of the control experiment. At an inhibitor concentration of  $0.10$  and  $1.00 \text{ mmol} \cdot \text{dm}^{-3}$ , the value of the corrosion current density near the free corrosion potential was reduced relative to the control. The degree of protection according to the polarization resistance method is  $\sim 70\%$ .



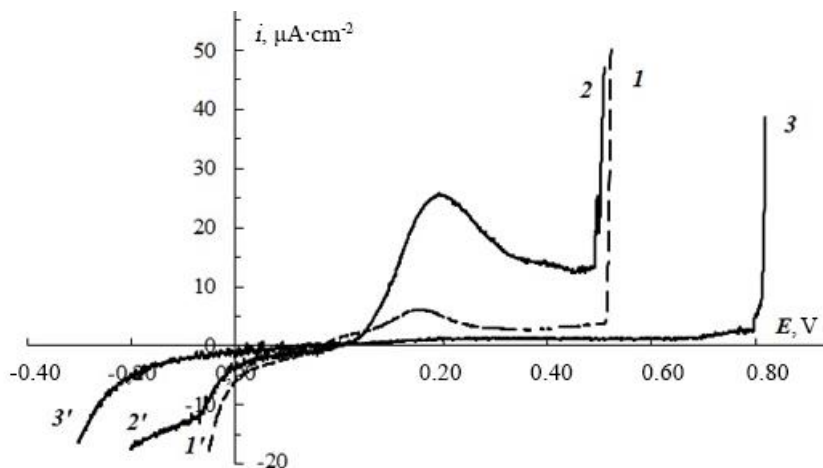
On cathodic polarization curves for inhibitor concentrations of  $0.10 \text{ mmol}\cdot\text{dm}^{-3}$  and  $1.00 \text{ mmol}\cdot\text{dm}^{-3}$ , an expansion of the region of small cathodic currents was observed (polarization curves were more compressed towards the current axis). The position of the increasing cathodic current density region was shifted by  $-180 \text{ mV}$  and  $-200 \text{ mV}$  relative to the control experiment, respectively. Thus, 1,2-(bis-[(5-amino-1*H*-1,2,4-triazol-3-yl)mercapto])ethane at a concentration of at least  $0.10 \text{ mmol}\cdot\text{dm}^{-3}$  can act as a mixed-type inhibitor.



**Figure 2.** Anodic ( $I-4$ ) and cathodic ( $I'-4'$ ) polarization curves of copper in borate buffer ( $\text{pH}=7.40$ ) with  $10 \text{ mM NaCl}$  and 1,2-(bis-[(5-amino-1*H*-1,2,4-triazol-3-yl)mercapto])ethane (**B**) at concentrations  $C_{\text{inh}}$  ( $\text{mmol}\cdot\text{dm}^{-3}$ ): 1,  $I'$  – without an inhibitor; 2,  $2'$  –  $0.01$ ; 3,  $3'$  –  $0.10$ ; 4,  $4'$  –  $1.00$ .

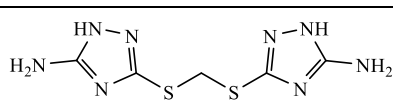
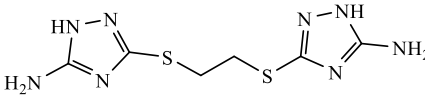
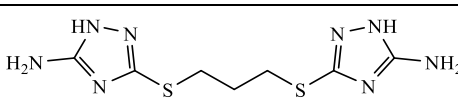
In the presence of  $0.01 \text{ mmol}\cdot\text{dm}^{-3}$   $\text{mmol}\cdot\text{dm}^{-3}$  of 1,3-bis[(5-amino-1*H*-1,2,4-triazol-3-yl)mercapto]propane **C**, a shift of the free corrosion potential by  $45 \text{ mV}$  towards the anodic direction was observed relative to the control value. At a concentration of  $0.10 \text{ mmol}\cdot\text{dm}^{-3}$ , the potential shift was  $5 \text{ mV}$  towards the cathodic direction. At an inhibitor concentration of  $0.01 \text{ mmol}\cdot\text{dm}^{-3}$ , a maximum anodic current density was observed on the anodic polarization curve, shifted by  $30 \text{ mV}$  towards the anodic direction relative to the control experiment, while at a concentration of  $0.10 \text{ mmol}\cdot\text{dm}^{-3}$ , no maximum was formed. The passivation current density for a concentration of  $0.01 \text{ mmol}\cdot\text{dm}^{-3}$  exceeded the values of the control experiment by 5 times, whereas for a concentration of  $0.10 \text{ mmol}\cdot\text{dm}^{-3}$ , it was reduced by a factor of 5. The value of the electrode potential at which the anodic current sharply increased was  $+690 \text{ mV}$  for a concentration of  $0.01 \text{ mmol}\cdot\text{dm}^{-3}$  and  $+1000 \text{ mV}$  for a concentration of  $0.10 \text{ mmol}\cdot\text{dm}^{-3}$ , with no visible pitting on the electrode surface. At inhibitor concentrations of  $0.01$  and  $0.10 \text{ mmol}\cdot\text{dm}^{-3}$ , the corrosion current density near the free corrosion potential decreased relative to the control. The degree of protection according to the polarization resistance method was approximately  $77\%$  and  $84\%$ , respectively. On the cathodic polarization curves, an expansion of the region of small cathodic currents was observed for an additive concentration of  $0.10 \text{ mmol}\cdot\text{dm}^{-3}$  (the polarization curve was compressed to the current axis). The position of the region of increasing cathodic current density was shifted

by  $-160$  mV relative to the control experiment. The cathodic polarization curve with the addition of  $0.01 \text{ mmol}\cdot\text{dm}^{-3}$  was within the experimental error range of the control. Therefore, 1,3-(bis-[(5-amino-1*H*-1,2,4-triazol-3-yl)mercapto])propane at a concentration of  $0.10 \text{ mmol}\cdot\text{dm}^{-3}$  can be a highly effective inhibitor of a mixed type.



**Figure 3.** Anodic ( $I-3$ ) and cathodic ( $I'-3'$ ) polarization curves of copper in borate buffer ( $\text{pH}=7.40$ ) with  $10 \text{ mM NaCl}$  and 1,3-(bis-[(5-amino-1*H*-1,2,4-triazol-3-yl)mercapto])propane (**C**) at concentrations  $C_{\text{inh}}$  ( $\text{mmol}\cdot\text{dm}^{-3}$ ):  $1, I'$  – without an inhibitor;  $2, 2'$  –  $0.01$ ;  $3, 3'$  –  $0.10$ .

**Table 3.** Open circuit potential, corrosion current density, and degree of protection of copper electrode in  $0.01 \text{ M NaCl}$  solutions with inhibitors studied.

Inhibitor	$C_{\text{inh}}, \text{mmol}\cdot\text{dm}^{-3}$	$E_{\text{cor}}, \text{V}$	$i_{\text{cor}}, \mu\text{A}\cdot\text{cm}^{-2}$	$Z_i, \%$
None	–	0.176	$1.2\pm 0.3$	–
 <b>A</b>	0.01	0.145	$3.7\pm 1.1$	$-208.33$
	0.10	0.147	$0.83\pm 0.19$	30.83
	1.00	0.120	$0.19\pm 0.05$	84.17
 <b>B</b>	0.01	0.155	$2.5\pm 0.9$	$-108.33$
	0.10	0.120	$0.36\pm 0.04$	70.00
	1.00	0.120	$0.36\pm 0.12$	70.00
 <b>C</b>	0.01	0.220	$0.27\pm 0.11$	77.50
	0.10	0.170	$0.19\pm 0.10$	84.17

Thus, the results of electrochemical corrosion tests indicate that the synthesized bis-triazolyl-mercapto-alkanes exhibit a moderate protective effect against copper corrosion at concentrations of at least  $0.10 \text{ mmol}\cdot\text{dm}^{-3}$ . Furthermore, the protective characteristics increased with the length of the linker hydrocarbon fragment. Similar results were obtained

in direct corrosion tests, which additionally demonstrate the influence of the hydrocarbon linker length on the protective characteristics of the inhibitor molecule.

Scientific publications dedicated to the study of inhibitors of the 5-amino-1*H*-1,2,4-triazole class extensively describe the formation of adsorbed layers of derivatives of this class on the surface of metals. Most scientists agree that the sorption of 5-amino-1*H*-1,2,4-triazoles on the surface of copper occurs through a combination of physical adsorption and chemical coordination involving hydrogen bonds and Van der Waals forces, as well as the formation of coordination bonds between the triazole molecule and copper. The endocyclic NH– and exocyclic NH<sub>2</sub>– groups are the primary binding sites in this mechanism [25–27]. In light of these findings, the cross-linked inhibitors synthesized in this work likely form protective films on the metal surface through a similar mechanism, with the only difference being that the number of potential binding centers in their molecule is twice as high. In this case, the fundamental scheme of inhibitor binding to the surface can be illustrated by Figure 4. This interpretation of the inhibitor sorption mechanism further explains the effect of increasing the length of the linker fragment on the inhibitory ability – as its length increases, the distance between heterocycles increases, steric hindrances for their coordination on the metal surface decrease, and hypothetically, the area of the protected surface per molecule of inhibitor increases.

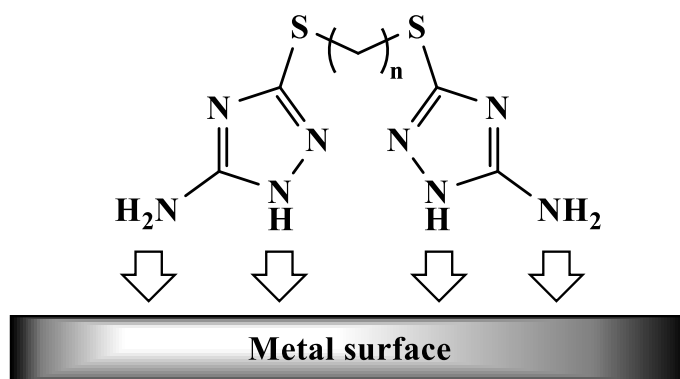


**Figure 4.** The basic scheme of self-organization of protective layers of bis-triazolyl-mercapto-alkanes on the surface of metal.

#### 4. Conclusion

Thus, as a result of the condensation of 3-mercapto-5-amino-1,2,4-triazole with dihaloalkanes, a series of bis-[(5-amino-1*H*-1,2,4-triazol-3-yl)thio]alkanes was obtained. Their inhibiting ability towards copper chloride corrosion was studied using a combination of direct and electrochemical methods. It was found that at concentrations of no less than 0.10 mmol·dm<sup>-3</sup>, bis-[(5-amino-1*H*-1,2,4-triazol-3-yl)thio]alkanes **A–C** exhibit extremely high protective characteristics both in direct tests (from 64 to 192 hours in salt mist and from 92 to 99% in 1 wt.% HCl solutions) and in electrochemical tests (from ~30 to ~85% in 10 mM NaCl solutions). The best anti-corrosion activity was observed for 1,3-bis-[(5-amino-

1*H*-1,2,4-triazol-3-yl)thio]propane **C**, which contains the longest linker aliphatic fragment among the studied substances.

These research results confirm the feasibility of further using the concept of twin molecules in the molecular design of new organic corrosion inhibitors. The chemical structure of the heterocyclic corrosion inhibitor double molecules can be improved in terms of the length and structure of the linker fragment, as well as the modification of the heterocyclic matrices and their side substituents. All of this opens up a wide synthetic and research space for the development of new highly effective corrosion inhibitors in the future.

### Acknowledgments

This work was supported by the Ministry of Science and Higher Education of the Russian Federation under the state assignment to universities for research activities in 2022–2024, project number FZGU-2022-0003.

### References

1. G. Kear, B.D. Barker and F.C. Walsh, Electrochemical corrosion of unalloyed copper in chloride media – a critical review, *Corros. Sci.*, 2004, **46**, no. 1, 109–135. doi: [10.1016/S0010-938X\(02\)00257-3](https://doi.org/10.1016/S0010-938X(02)00257-3)
2. F. Ammeloot, C. Fiaud and E.M.M. Sutter, Characterization of the oxide layers on a Cu 13Sn alloy in a NaCl aqueous solution without and with 0.1 M benzotriazole. Electrochemical and photoelectrochemical contributions, *Electrochim. Acta*, 1999, **44**, no. 15, 2549–2558. doi: [10.1016/S0013-4686\(98\)00391-0](https://doi.org/10.1016/S0013-4686(98)00391-0)
3. M. Finšgar and I. Milošev, Inhibition of copper corrosion by 1,2,3-benzotriazole: A review, *Corros. Sci.*, 2010, **52**, no. 9, 2737–2749. doi: [10.1016/j.corsci.2010.05.002](https://doi.org/10.1016/j.corsci.2010.05.002)
4. Yu.I. Kuznetsov and L.P. Kazanskiy, Physicochemical aspects of metal protection by azoles as corrosion inhibitors, *Russ. Chem. Rev.*, 2008, **77**, no. 3, 219–232. doi: [10.1070/rc2008v077n03abeh003753](https://doi.org/10.1070/rc2008v077n03abeh003753)
5. Yu.I. Kuznetsov, Kh.S. Shikhaliev, M.O. Agafonkina, N.P. Andreeva, I.A. Arkhipushkin, A.Yu. Potapov and L.P. Kazansky, Effect of substituents in 5-R-3-amino-1, 2, 4-triazoles on the chemisorption on copper surface in neutral media, *Corros. Eng., Sci. Technol.*, 2021, **56**, no. 1, 60–70. doi: [10.1080/1478422X.2020.1807087](https://doi.org/10.1080/1478422X.2020.1807087)
6. Yu.I. Kuznetsov, New possibilities of metal corrosion inhibition by organic heterocyclic compounds, *Int. J. Corros. Scale Inhib.*, 2012, **1**, no. 1, 3–15. doi: [10.17675/2305-6894-2012-1-1-003-015](https://doi.org/10.17675/2305-6894-2012-1-1-003-015)
7. H.O. Curkovic, E. Stupnisek-Lisac and H. Takenouti, Electrochemical quartz crystal microbalance and electrochemical impedance spectroscopy study of copper corrosion inhibition by imidazoles, *Corros. Sci.*, 2009, **51**, no. 10, 2342–2348. doi: [10.1016/j.corsci.2009.06.018](https://doi.org/10.1016/j.corsci.2009.06.018)
8. P. Dupin, A. de Savignac and A. Lattes, Free and Wilson correlation between the molecular structure of some imidazolines and their corrosion inhibiting properties, *Mater. Corros.*, 1982, **33**, no. 4, 203–206. doi: [10.1002/maco.19820330404](https://doi.org/10.1002/maco.19820330404)

9. Y. Derbali, M. Duprat, A. Lattes and A. de Savignac, Propriétés inhibitrices de corrosion de monoalkyl phosphates et phosphonates disodiques, *J. Soc. Chim. Tunis.*, 1986, **2**, no. 3, 35–41.
10. G. Schmitt, Proceedings of the Sixth European Symposium on Corrosion Inhibitors, *Ann. Univ. Ferrara, Sez.*, 1985, no. 8.
11. F. Dabosi, Y. Derbali, M. Etman, A. Srhiri and A. de Savignac, Influence of some organic compounds on the corrosion mechanism of carbon steel (XC<sub>38</sub>) in 3% NaCl I. dodecyl sodium phosphonate (C<sub>10</sub>H<sub>21</sub>PO<sub>3</sub>Na<sub>2</sub>) and n-undecylimidazole (C<sub>14</sub>H<sub>26</sub>N<sub>2</sub>) surfactants, *J. Appl. Electrochem.*, 1991, **21**, 255–260. doi: [10.1007/BF01052579](https://doi.org/10.1007/BF01052579)
12. M.El Achouri, M.S. Hajji, S. Kertit, M. Essassi, M. Salem and R. Coudert, Some surfactants in the series of 2-(alkyldimethylammonio) alkanol bromides as inhibitors of the corrosion of iron in acid chloride solution, *Corros. Sci.*, 1995, **37**, no. 3, 381–389. doi: [10.1016/0010-938X\(94\)00134-R](https://doi.org/10.1016/0010-938X(94)00134-R)
13. R.J. Meakins, Alkyl quaternary ammonium compounds as inhibitors of the acid corrosion of steel, *J. Appl. Chem.*, 1963, **13**, no. 8, 339–345. doi: [10.1002/jctb.5010130803](https://doi.org/10.1002/jctb.5010130803)
14. T. Vasudevan, S. Muralidharan, S. Alwarappan and S.V.K. Iyer, The influence of N-hexadecyl benzyl dimethyl ammonium chloride on the corrosion of mild steel in acids, *Corros. Sci.*, 1995, **37**, no. 8, 1235–1244. doi: [10.1016/0010-938X\(95\)00028-I](https://doi.org/10.1016/0010-938X(95)00028-I)
15. A. Frignani, M. Tassinari and G. Trabaneli, Impedance measurements on Armco iron in acid solution inhibited by S-containing additives, *Electrochim. Acta*, 1989, **34**, no. 8, 1259–1263. doi: [10.1016/0013-4686\(89\)87168-3](https://doi.org/10.1016/0013-4686(89)87168-3)
16. F.M. Menger and C.A. Littau, Gemini-surfactants: synthesis and properties, *J. Am. Chem. Soc.*, 1991, **113**, no. 4, 1451–1452. doi: [10.1021/ja00004a077](https://doi.org/10.1021/ja00004a077)
17. F.M. Menger and C.A. Littau, Gemini surfactants: a new class of self-assembling molecules, *J. Am. Chem. Soc.*, 1993, **115**, no. 22, 10083–10090. doi: [10.1021/ja00075a025](https://doi.org/10.1021/ja00075a025)
18. R. Zana, M. Benrraou and R. Rueff, Alkanediyl-.alpha.,.omega.-bis (dimethylalkylammonium bromide) surfactants. 1. Effect of the spacer chain length on the critical micelle concentration and micelle ionization degree, *Langmuir*, 1991, **7**, no. 6, 1072–1075. doi: [10.1021/la00054a008](https://doi.org/10.1021/la00054a008)
19. R. Zana, Gemini (dimeric) surfactants, *Curr. Opin. Colloid Interface Sci.*, 1996, **1**, no 5, 566–571. doi: [10.1016/S1359-0294\(96\)80093-8](https://doi.org/10.1016/S1359-0294(96)80093-8)
20. B. Brycki and A. Szulc, Gemini surfactants as corrosion inhibitors. A review, *J. Mol. Liq.*, 2021, **344**, 117686. doi: [10.1016/j.molliq.2021.117686](https://doi.org/10.1016/j.molliq.2021.117686)
21. F.E.T. Heakal and A.E. Elkholy, Gemini surfactants as corrosion inhibitors for carbon steel, *J. Mol. Liq.*, 2017, **230**, 395–407. [10.1016/j.molliq.2017.01.047](https://doi.org/10.1016/j.molliq.2017.01.047)
22. A.A. Kruzhilin, D.S. Shevtsov, A.Y. Potapov, K.S. Shikhaliev, O.A. Kozaderov, C. Prabhakar and V.E. Kasatkin, Novel inhibitory compositions based on 4, 5, 6, 7-tetrahydro-[1, 2, 4] triazolo [1, 5-a] pyrimidin-7-ol derivatives for steel acid corrosion protection, *Int. J. Corros. Scale Inhib.*, 2022, **11**, no. 2, 774–795. doi: [10.17675/2305-6894-2022-11-2-22](https://doi.org/10.17675/2305-6894-2022-11-2-22)

- 
23. O.A. Kozaderov, K.S. Shikhaliev, C. Prabhakar, A. Tripathi, D.S. Shevtsov, A.A. Kruzhilin, E.V. Komarova and Y.I. Kuznetsov, Corrosion of  $\alpha$ -Brass in Solutions Containing Chloride Ions and 3-Mercaptoalkyl-5-amino-1*H*-1,2,4-triazoles, *Appl. Sci.*, 2019, **9**, no. 14, 2821. doi: [10.3390/app9142821](https://doi.org/10.3390/app9142821)
  24. F. Mansfeld, Tafel slopes and corrosion rates obtained in the pre-Tafel region of polarization curves, *Corros. Sci.*, 2005, **47**, no. 12, 3178–3186. doi: [10.1016/j.corsci.2005.04.012](https://doi.org/10.1016/j.corsci.2005.04.012)
  25. H.H. Hassan, E. Abdelghani and M.A. Amin, Inhibition of mild steel corrosion in hydrochloric acid solution by triazole derivatives: Part I. Polarization and EIS studies, *Electrochim. Acta*, 2007, **52**, no. 22, 6359–6366. doi: [10.1016/j.electActa2007.04.046](https://doi.org/10.1016/j.electActa2007.04.046)
  26. M.K. Awad, M.R. Mustafa and M.M.A. Elnga, Computational simulation of the molecular structure of some triazoles as inhibitors for the corrosion of metal surface, *J. Mol. Struct.: THEOCHEM*, 2010, **959**, no. 1–3, 66–74. doi: [10.1016/j.theochem.2010.08.008](https://doi.org/10.1016/j.theochem.2010.08.008)
  27. A. Lesar and I. Milošev, Density functional study of the corrosion inhibition properties of 1,2,4-triazole and its amino derivatives, *Chem. Phys. Lett.*, 2009, **483**, no. 4–6, 198–203. doi: [10.1016/j.cplett.2009.10.082](https://doi.org/10.1016/j.cplett.2009.10.082)

